Electronic Supporting Information

to

Biogeochemical and Hydrologic Synergy Controls Mercury Fate in an Arid Land River-Reservoir System

Brett A. Poulin[1*], Michael T. Tate[2], Jacob Ogorek[2], Sara E. Breitmeyer[3], Austin K. Baldwin[4], Alysa M. Yoder[4], Reed Harris[5], Jesse Naymik[6], Nick Gastelecutto[6], Charles Hoovestol[6], Christopher Larsen[6], Ralph Myers[6], George R. Aiken[7], David P. Krabbenhoft[2]

[1]Department of Environmental Toxicology, University of California, Davis
[2]U.S. Geological Survey, Upper Midwest Water Science Center
[3]U.S. Geological Survey, New Jersey Water Science Center
[4]U.S. Geological Survey, Idaho Water Science Center
[5]Reed Harris
[6]Idaho Power Company
[7]U.S. Geological Survey, Water Mission Area, USA

* Corresponding author. Tel: +1 530 754 2454. *Email address:* bapoulin@ucdavis.edu

Electronic supporting information includes 2 Tables, 15 Figures, electronic annimations of Figures S6-S13, and 21 pages.

Section S1. Volume Weighted Average Calculations for Brownlee Reservoir

Volume-weighted average concentrations of divalent inorganic Hg (Hg(II)) and methylmercury (MeHg) were determined for the combined epilimnion and metalimnion at three sites within Brownlee Reservoir in 2017 and 2018. In the analysis, volume-weighted averages were determined at each of the three sites (Snake River miles 318, 300, and 286) as a function of water depth, as opposed to the entire water body. The goals of this analysis were to assess the spatial and temporal dynamics of particulate methylmercury (p.MeHg) andparticulate Hg(II) (p.Hg(II)) within Brownlee Reservoir and ascertain the drivers for shifts in Hg distribution between Brownlee inflow and outflow locations (Snake River miles 346 and 284, respectively). This analysis focused on Hg on particles in the epilimnion and metalimnion for two reasons: particles in these water layers are (1) transported laterally in the reservoir and exported via the penstocks[1,2] and (2) the association of MeHg with particles is a proxy for MeHg uptake at the base of the aquatic food web. An additional rationale to exclude particle measurements in the hypolimnion is that the low particle density of this strata yielded extremely high Hg concentrations, which would bias volume-weighted particle concentrations. Limnologic layers were defined using temperature profiles collected simultaneously with discrete water sample collection,[3] using similar methodology as a separate study of the reservoir system.[4] Multiple samples were collected across the epilimnion and metalimnion (detailed in *Water Sample Collection* subsection of the main text). Volume-weighted averages were calculated by summing discrete concentrations of p.Hg(II) and p.MeHg multiplied by the percentage each measurement represented across the water column of the epilimnion and metalimnion; this was carried out for each water profile of unique sampling events, and using both volumetric and gravimetric concentrations of p.Hg(II) and p.MeHg. As such, Table S2 presents the summary data of volume-weighted constituents in the epilimnion and metalimnion in 2017 and 2018.

Section S2. Tables

Table S1. Date ranges defined as “high flow” conditions based on daily discharge at the inflow to Brownlee Reservoir (Snake River Mile 346, USGS Gauge ID 132692001); all other dates were considered base-flow conditions. The table includes the start and conclusion of reservoir destratification based on measurements of temperature.[3] The hydrographs for each year of the study are presented in Figure S1.

Calendar Year	Start Date, High Flow	Stop Date, High Flow	Start of Destratification Period	Conclusion of Destratification Period
2014	2/1	7/18	--	--
2015	2/1	6/20	--	--
2016	1/26	7/1	7/24/2016	12/30/2016
2017	1/8	7/4	7/11/2017	12/31/2017
2018	2/1	6/15	7/31/2018	12/11/2018
2019	2/1	7/7	7/18/2019	12/13/2019
2020	2/1	7/1	8/4/2020	12/31/2020

– indicates data are not available.

Table S2. Volume-weighted constituent concentrations (DOC, p.MeHg, p.Hg(II)), DOM properties (α_{254}, $SUVA_{254}$, $S_{275-295}$) and distribution coefficients (log K_d Hg(II), log K_d MeHg) for the epilimnion and metalimnion of Brownlee Reservoir (2017, 2018).[3]

Site	Date	DOC (mgC L^{-1})	α_{254} (cm^{-1})	$SUVA_{254}$ (L mgC^{-1} m^{-1})	$S_{275-295}$ ($x10^{-3}$ nm^{-1})	Vol. p.MeHg (ng L^{-1})	Grav. p.MeHg (ng g^{-1})	Vol. p.Hg(II) (ng L^{-1})	Grav. p.Hg(II) (ng g^{-1})	logK_d MeHg (L kg^{-1})	logK_d Hg(II) (L kg^{-1})
286	3/20/2017	3.33	0.12	3.54	13.97	0.03	2.31	1.12	90.02	4.91	4.82
286	5/1/2017	3.03	0.09	2.94	14.96	0.04	3.56	1.44	143.10	5.28	4.96
286	6/5/2017	3.17	0.08	2.52	15.62	0.04	6.44	0.38	66.37	4.87	4.95
286	7/25/2017	3.33	0.08	2.35	16.09	0.04	10.27	0.46	190.14	5.47	5.26
286	8/23/2017	3.03	0.07	2.41	16.18	0.04	28.77	0.22	172.10	5.60	5.53
286	9/25/2017	2.96	0.07	2.40	16.37	0.17	62.31	0.25	100.81	4.71	5.38
286	11/14/2017	2.52	0.05	1.99	15.58	0.04	14.01	0.33	114.55	5.62	5.55
286	4/12/2018	2.50	0.06	2.30	15.74	0.04	5.83	0.42	55.08	5.24	5.21
286	5/1/2018	--	--	--	--	0.04	5.32	--	--	--	5.07
286	5/22/2018	2.70	0.06	2.20	16.90	0.02	4.41	--	--	--	5.15
286	6/18/2018	2.52	0.06	2.31	16.09	0.00	3.62	0.19	154.05	5.47	4.74
286	7/31/2018	4.00	0.07	1.70	19.70	0.02	4.95	0.52	123.00	5.59	--
286	8/22/2018	2.62	0.06	2.21	17.02	0.01	14.07	0.33	307.43	6.14	5.45
286	9/11/2018	2.90	0.06	2.21	16.78	0.04	30.52	0.30	218.90	5.66	5.51
286	9/24/2018	2.65	0.06	2.12	16.66	0.06	101.57	0.13	439.44	4.83	4.70
286	10/16/2018	2.41	0.05	2.23	17.13	0.05	43.25	0.13	112.08	5.56	5.84
286	11/6/2018	2.60	0.05	2.12	16.42	0.02	17.34	0.11	87.35	5.54	5.65
286	11/27/2018	2.30	0.05	2.00	16.40	0.03	22.50	0.11	90.80	5.52	5.86
286	12/11/2018	2.20	0.04	1.88	15.18	0.06	37.78	0.10	65.64	5.35	5.62
300	3/20/2017	3.58	0.13	3.48	14.79	0.05	1.39	2.51	74.60	4.80	4.76
300	5/1/2017	3.02	0.10	3.21	15.34	0.06	2.04	2.66	95.89	4.96	4.77
300	6/6/2017	3.02	0.08	2.77	15.31	0.05	6.75	0.50	65.00	4.95	4.97
300	7/25/2017	3.20	0.08	2.42	15.77	0.06	25.22	0.57	237.70	5.64	5.26
300	8/23/2017	3.21	0.07	2.27	16.45	0.11	58.80	0.33	175.25	5.50	5.42
300	9/26/2017	3.12	0.07	2.16	16.44	0.09	18.59	0.32	57.29	4.98	4.97
300	11/14/2017	2.53	0.05	1.97	15.63	0.02	6.80	0.33	101.67	5.53	5.40
300	4/12/2018	2.56	0.06	2.34	15.21	0.07	5.51	0.60	49.14	5.16	5.07
300	5/1/2018	2.47	0.05	2.07	15.77	0.05	5.89	--	--	--	5.20
300	5/22/2018	2.60	0.06	2.30	16.80	0.04	6.91	--	--	--	5.11
300	6/18/2018	2.57	0.06	2.20	16.17	0.02	9.40	0.22	90.43	5.27	5.03
300	7/10/2018	2.50	0.06	2.33	16.39	0.04	40.60	0.32	309.92	5.95	5.67
300	7/31/2018	2.66	0.06	2.08	17.21	0.03	25.51	0.36	349.41	6.12	5.74

300	8/22/2018	2.80	0.06	2.15	16.99	0.02	11.53	0.51	336.65	6.15	5.27
300	9/11/2018	2.96	0.06	2.08	16.71	0.07	35.60	0.25	146.93	5.70	5.57
300	9/25/2018	2.86	0.06	2.06	16.78	0.09	94.69	0.19	303.39	4.51	5.70
300	10/16/2018	2.52	0.06	2.23	16.19	0.07	34.54	0.13	81.66	5.24	5.41
300	11/6/2018	2.51	0.05	2.04	16.03	0.14	47.50	0.20	80.73	4.57	5.58
300	11/27/2018	2.28	0.04	1.91	15.69	0.01	5.60	0.14	86.99	5.52	5.40
300	12/11/2018	2.36	0.04	1.87	15.41	0.01	5.53	0.16	67.44	5.44	5.41
310	3/20/2017	3.53	0.13	3.63	14.37	0.07	1.16	3.72	58.41	4.63	4.68
310	5/1/2017	3.03	0.10	3.24	15.28	0.06	1.42	2.50	56.26	4.82	4.68
310	6/8/2017	2.95	0.08	2.81	15.02	0.02	2.08	0.62	55.27	4.82	4.39
310	7/25/2017	3.35	0.09	2.55	15.45	0.01	1.87	1.02	210.84	5.59	3.81
310	8/23/2017	3.39	0.08	2.30	17.07	0.32	23.22	0.76	81.69	5.26	5.32
310	9/28/2017	3.00	0.06	2.17	16.47	0.06	7.35	0.41	38.00	5.10	5.36
310	11/14/2017	2.60	0.05	2.00	15.21	0.02	5.37	0.34	90.85	5.45	5.27
310	6/19/2018	2.71	0.06	2.25	17.03	0.19	51.45	0.47	128.81	5.51	5.19
310	9/25/2018	3.13	0.06	1.93	17.02	0.05	12.20	0.54	60.92	5.23	5.11
318	3/20/2017	3.50	0.13	3.70	14.00	0.27	1.13	10.40	42.90	4.50	--
318	5/1/2017	3.10	0.10	3.10	15.30	0.19	1.25	7.80	51.30	4.76	4.74
318	6/8/2017	2.96	0.08	2.72	14.94	0.09	5.37	0.74	44.31	4.58	--
318	7/25/2017	3.34	0.08	2.41	15.33	0.13	8.38	0.81	69.67	3.99	--
318	8/23/2017	3.63	0.08	2.30	15.97	0.12	6.86	0.70	40.22	4.93	5.28
318	9/28/2017	2.99	0.06	2.07	16.30	0.05	3.85	0.49	34.99	4.89	5.09
318	11/14/2017	2.50	0.05	1.80	14.89	0.02	3.85	0.33	66.54	5.30	5.16
318	4/12/2018	2.70	0.06	2.35	15.12	0.15	2.81	2.46	45.68	4.93	4.91
318	5/1/2018	2.90	0.07	2.40	14.70	0.06	2.39	--	--	--	4.73
318	5/22/2018	2.60	0.06	2.50	15.10	0.07	4.77	--	--	--	5.08
318	6/19/2018	2.99	0.06	2.00	16.93	0.12	8.81	0.63	46.22	4.96	5.21
318	7/10/2018	3.21	0.07	2.24	16.91	0.06	11.63	0.49	95.27	5.37	5.24
318	7/31/2018	2.90	0.06	2.10	16.70	0.04	7.46	0.48	86.40	5.40	4.94
318	8/22/2018	3.20	0.07	2.10	16.20	0.04	7.05	0.29	56.40	5.24	4.87
318	9/11/2018	3.50	0.07	2.00	16.00	0.08	7.29	0.62	59.00	5.04	4.96
318	9/26/2018	3.11	0.06	1.85	16.20	0.12	6.25	0.29	29.11	4.77	4.87
318	10/16/2018	2.80	0.06	2.00	16.20	0.04	17.80	0.11	49.70	5.13	5.66
318	11/6/2018	2.50	0.05	2.00	14.70	0.01	2.70	0.26	57.80	5.30	5.00
318	11/27/2018	2.20	0.04	1.90	14.40	0.02	3.39	0.21	29.50	5.03	5.45
318	12/11/2018	2.50	0.04	1.70	14.00	0.04	4.45	0.25	27.70	4.89	--

– indicates data are not available. “Vol.” indicate volumetric. “Grav.” Indicates gravimetric.

Section S3. Figures

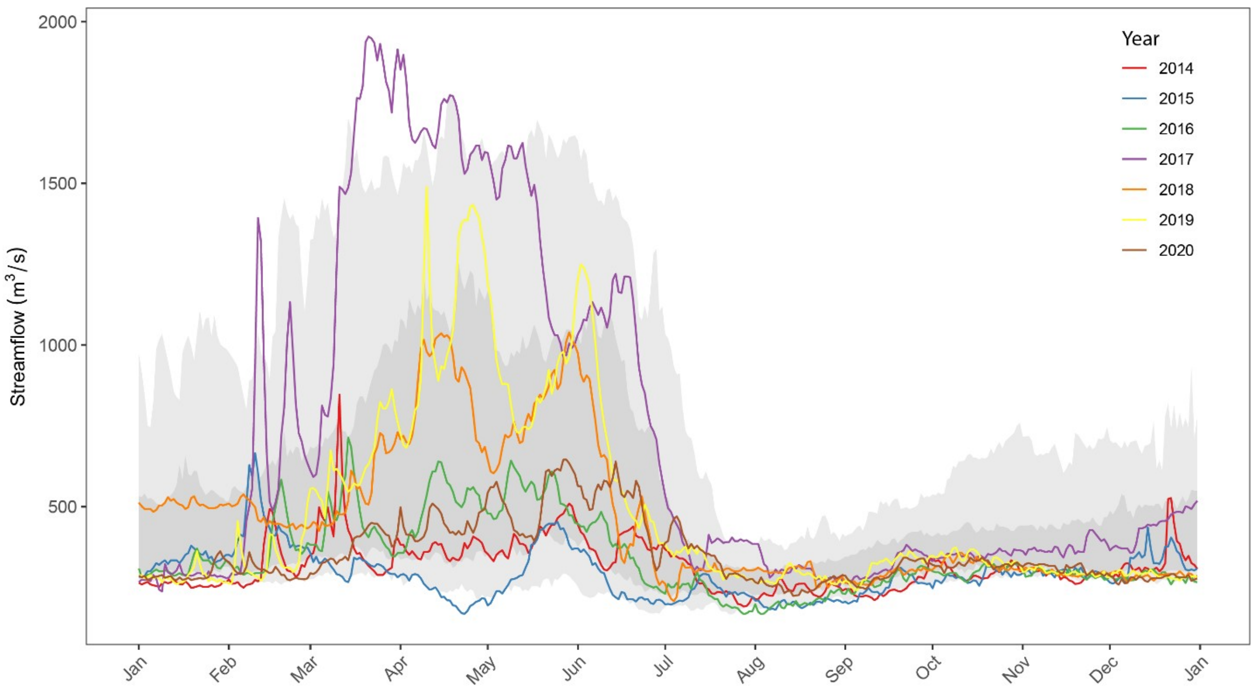

Figure S1. Daily mean streamflow of the Snake River at Weiser, ID, upstream of Brownlee Reservoir (USGS stream gage 13269000),[5] for the study years 2014 – 2020. For comparison, the light and dark shaded regions represent the 5th – 95th and 25th – 75th percentiles, respectively, of daily mean streamflow from 1968-2020.

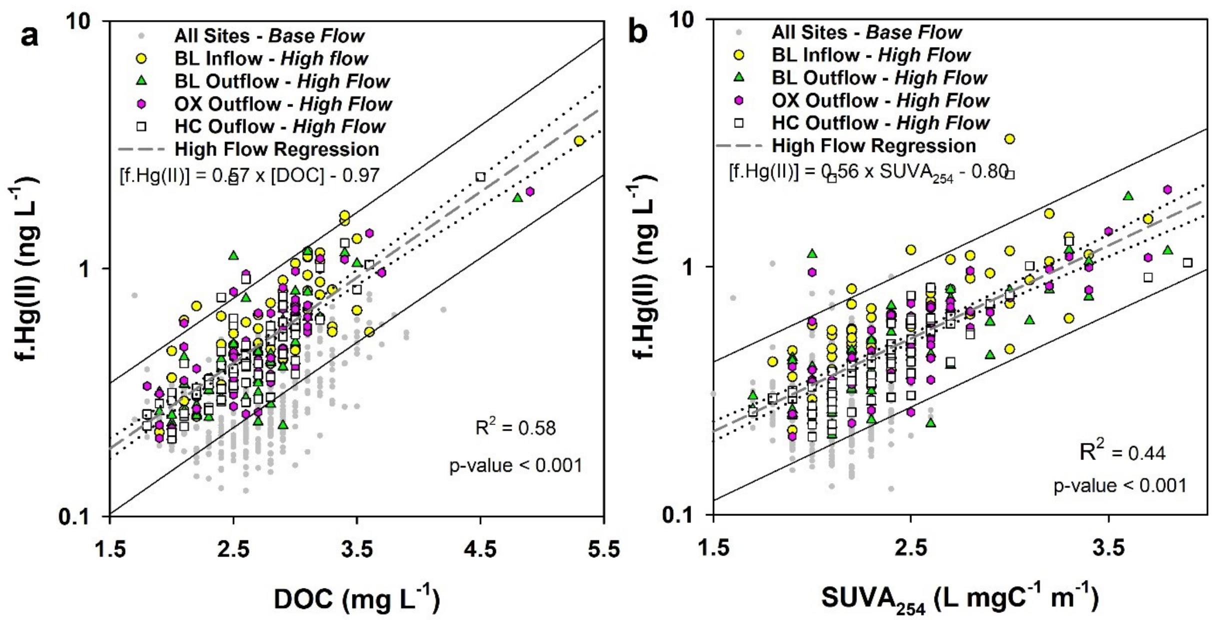

Figure S2. Scatter plots and linear regression lines between filter-passing Hg(II) and (a) dissolved organic carbon (DOC) concentration and (b) specific ultraviolet absorbance at 254 nm ($SUVA_{254}$) at inflow – outflow sites of the Hells Canyon Complex.[3] The dashed gray, dotted black, and solid black lines present the linear fit of data, 95% confidence interval of the fit, and prediction interval of the fit, respectively, for samples collected under high flow conditions (*n*=271; see Table S1 for date ranges).

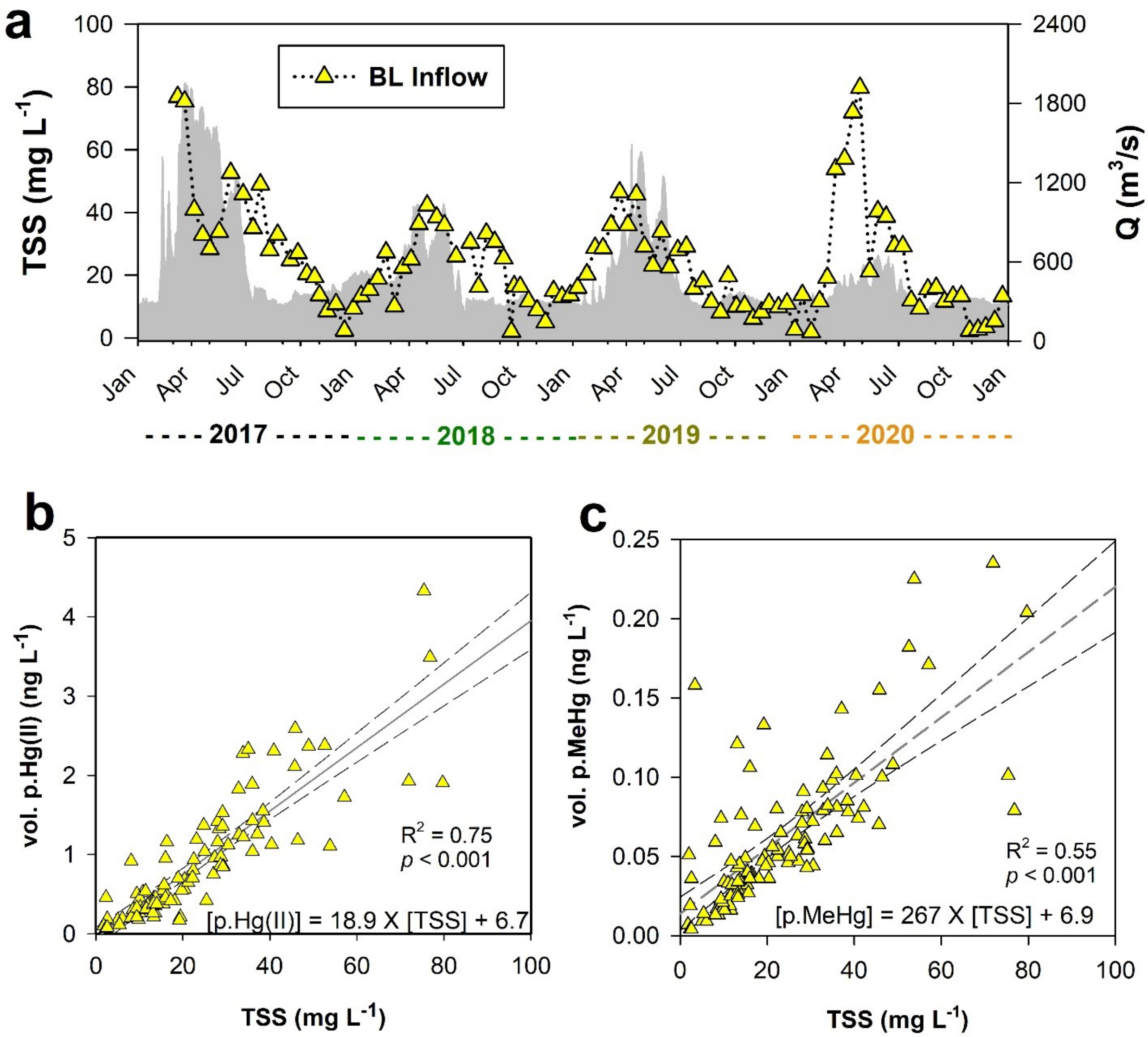

Figure S3. The concentrations of total suspended solids (TSS) at Brownlee Reservoir (BL) Inflow (2017 – 2020) and scatter plots and linear regressions between TSS and volumetric (b) particulate Hg(II) (p.Hg(II)) concentration and (c) particulate methylmercury (p.MeHg) concentration at Brownlee Reservoir Inflow.[3] The dashed gray and dashed black lines in plots b and c present the linear fit of data and 95% confidence interval of the fit, respectively, between 2017 – 2020 (n=104). Two outlier data points were omitted from the regression analyses (collected on 4/17/2018 and 6/19/2018) due to particulate values far outside the range of other samples during the study period.

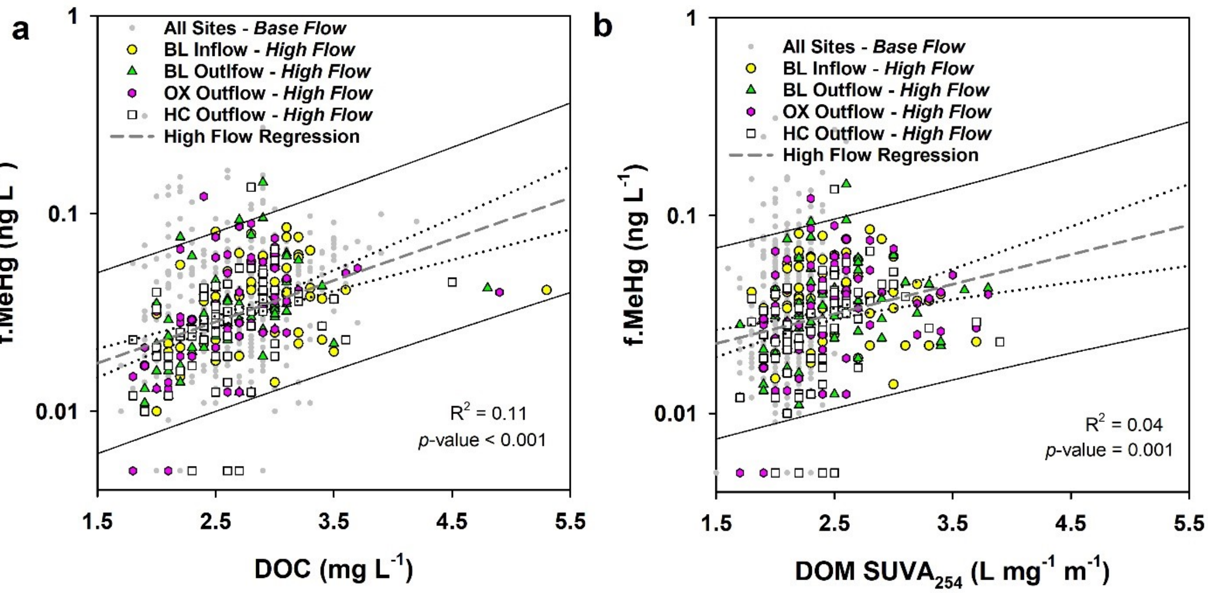

Figure S4. Scatter plots showing the low correlation between the concentration of dissolved organic carbon (DOC) or dissolved organic matter (DOM) specific ultraviolet absorbance ($SUVA_{254}$) and concentration of filter-passing methylmercury (f.MeHg) at reservoir inflow and outflow locations.[3]

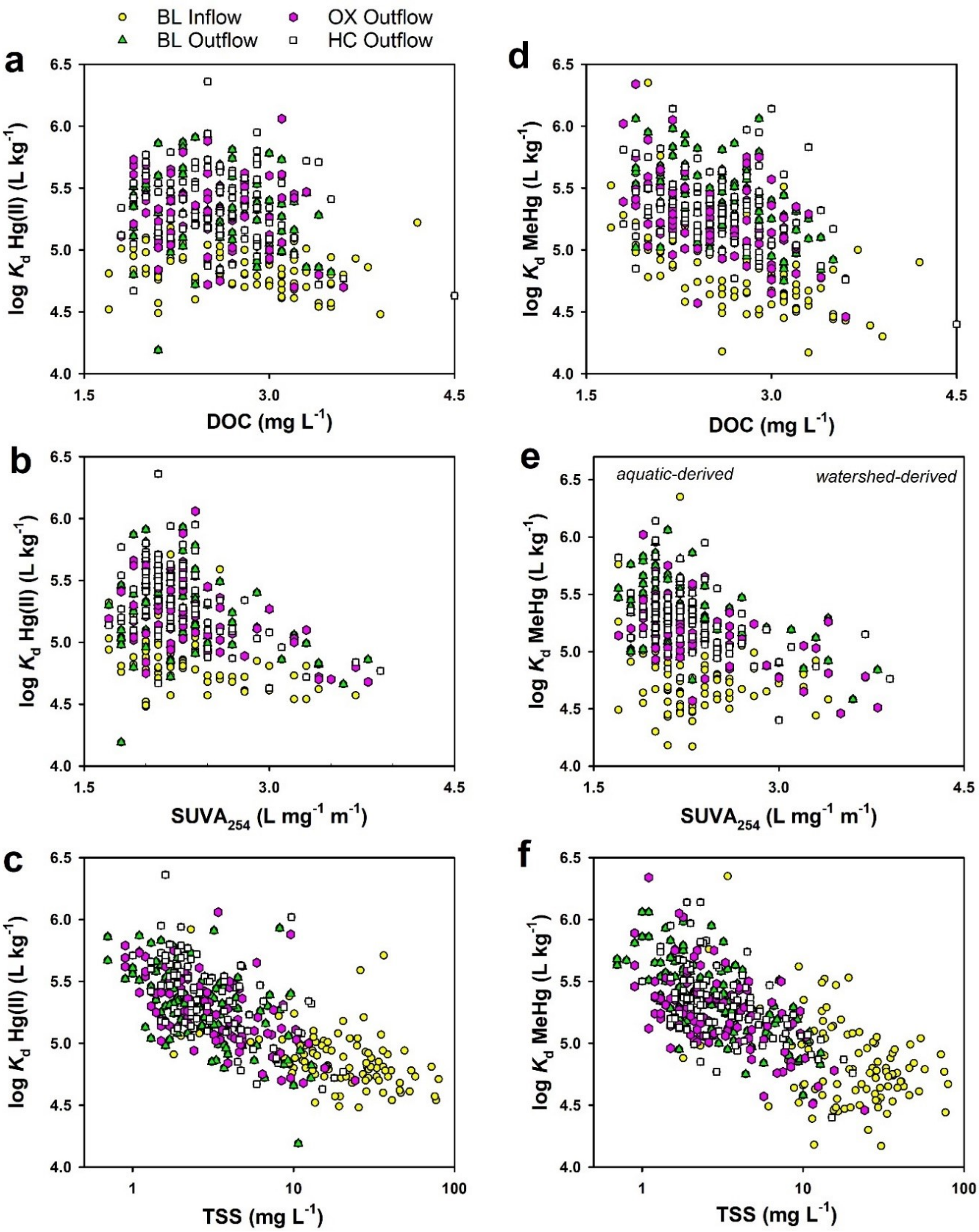

Figure S5. Scatter plots show the observed behavior between (a-c) log K_d Hg(II) and (d-f) log K_d MeHg and DOC concentration, DOM specific ultraviolet absorbance ($SUVA_{254}$), and the TSS from 2014 – 2020 at inflow – outflow sites of the Hells Canyon Complex (Brownlee Reservoir (BL) Inflow (*n*=102), Brownlee Reservoir Outflow (*n*=105), Oxbow Reservoir (OX) Outflow (*n*=100), and Hells Canyon Reservoir (HC) Outflow (*n*=101)).[3]

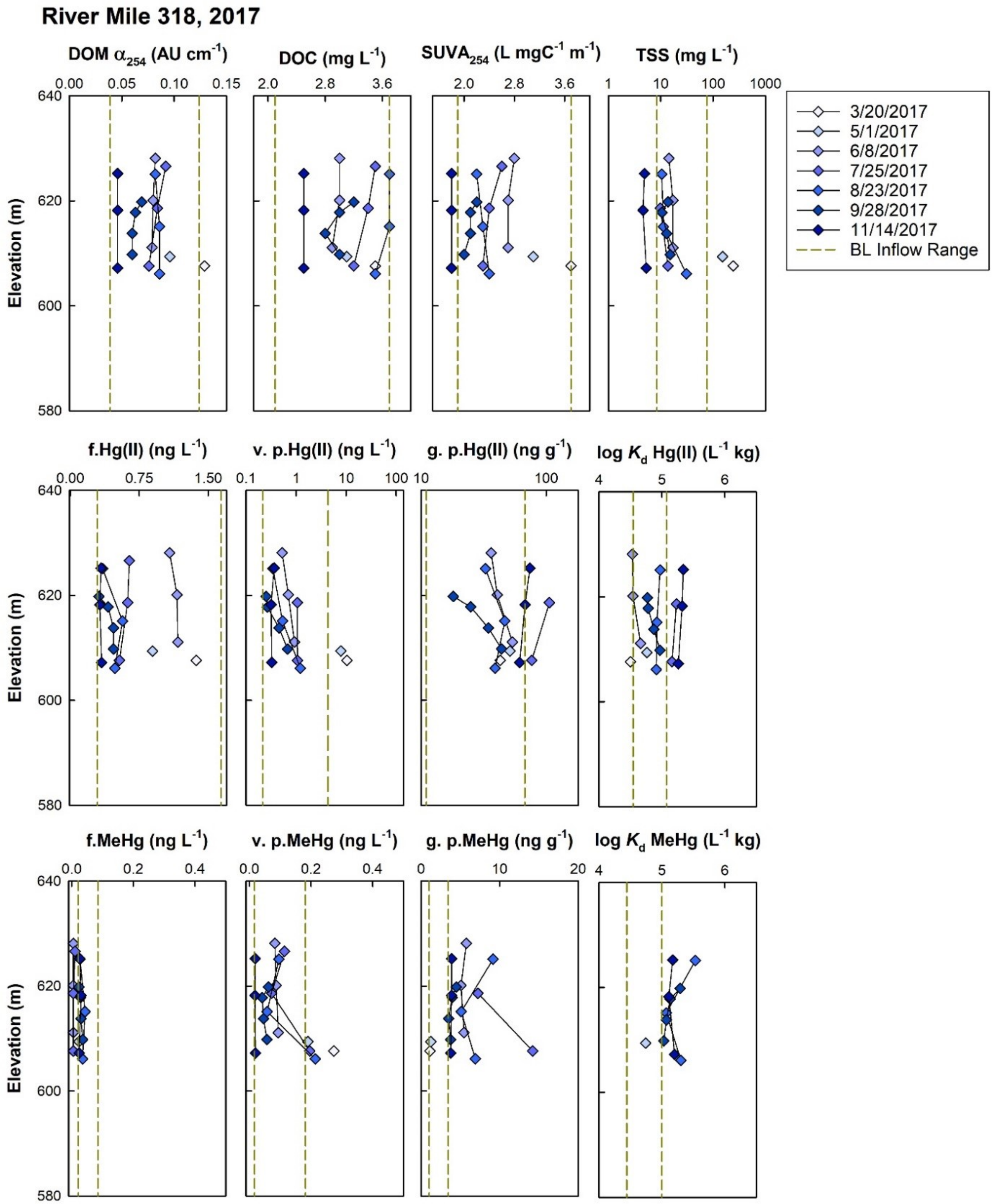

Figure S6. Depth profiles at river mile 318 in Brownlee Reservoir in 2017 of DOM α_{254}, DOC, SUVA$_{254}$, and TSS (top panel); f.Hg(II), vol. and grav. p.Hg(II) (ng L^{-1}, ng g^{-1}), and log K_d Hg(II) (middle panel); and f.MeHg, vol. and grav. p.MeHg (ng L^{-1}; ng g^{-1}), TSS and log K_d MeHg (bottom panel).[3] The sediment elevation at this location is 602.6 m. Dashed lines present the range of values observed at river mile 346 (BL Inflow) during the time frame.

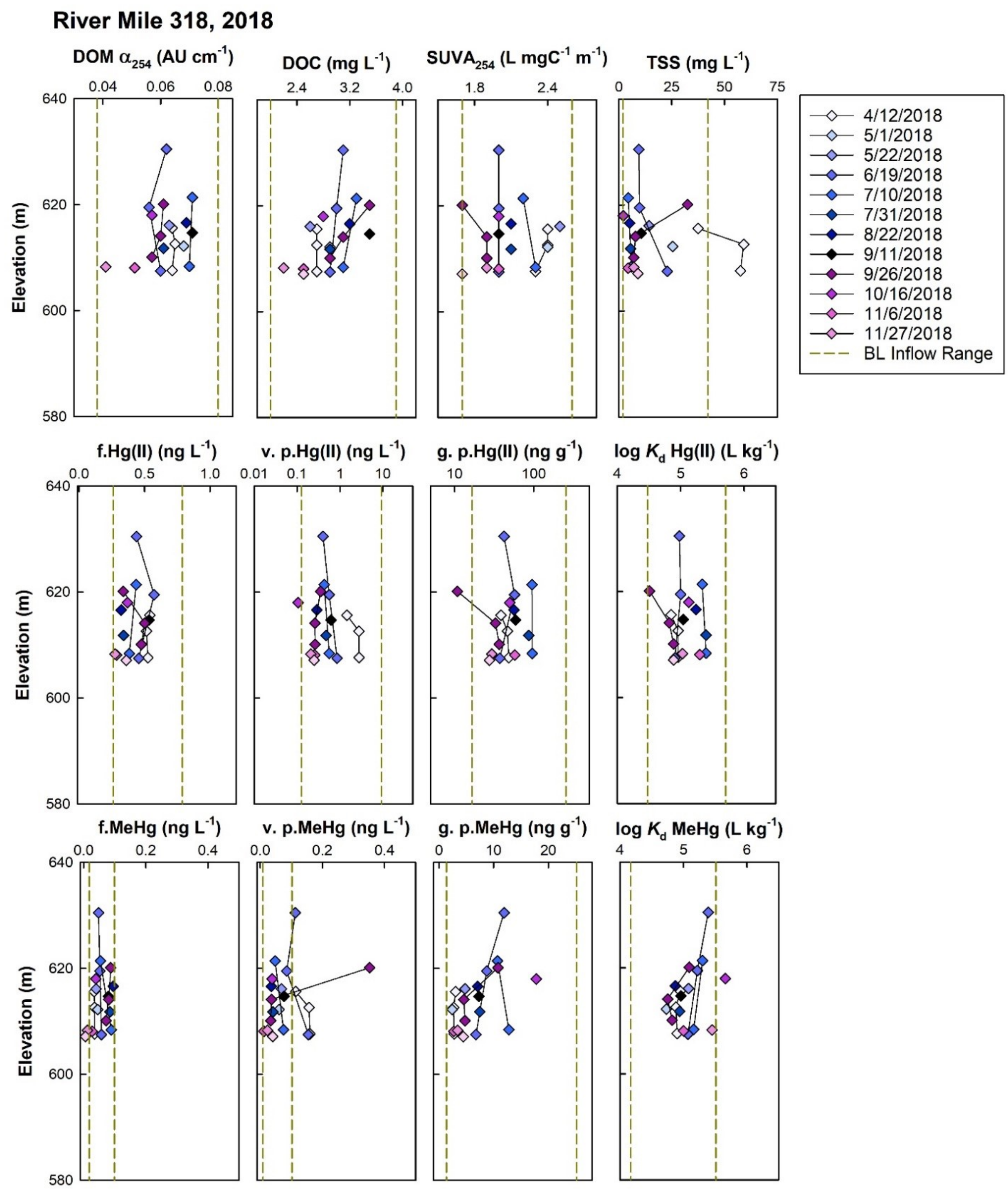

Figure S7. Depth profiles at river mile 318 in Brownlee Reservoir in 2018 of DOM α_{254}, DOC, $SUVA_{254}$, and [TSS] (top panel); f.Hg(II), vol. and grav. p.Hg(II) (ng L^{-1}, ng g^{-1}), and log K_d Hg(II) (middle panel); and f.MeHg, vol. and grav. p.MeHg (ng L^{-1}; ng g^{-1}), and log K_d MeHg (bottom panel).[3] The sediment elevation at this location was 602.6 m. Dashed lines present the range of values observed at river mile 346 (BL Inflow) during the time frame.

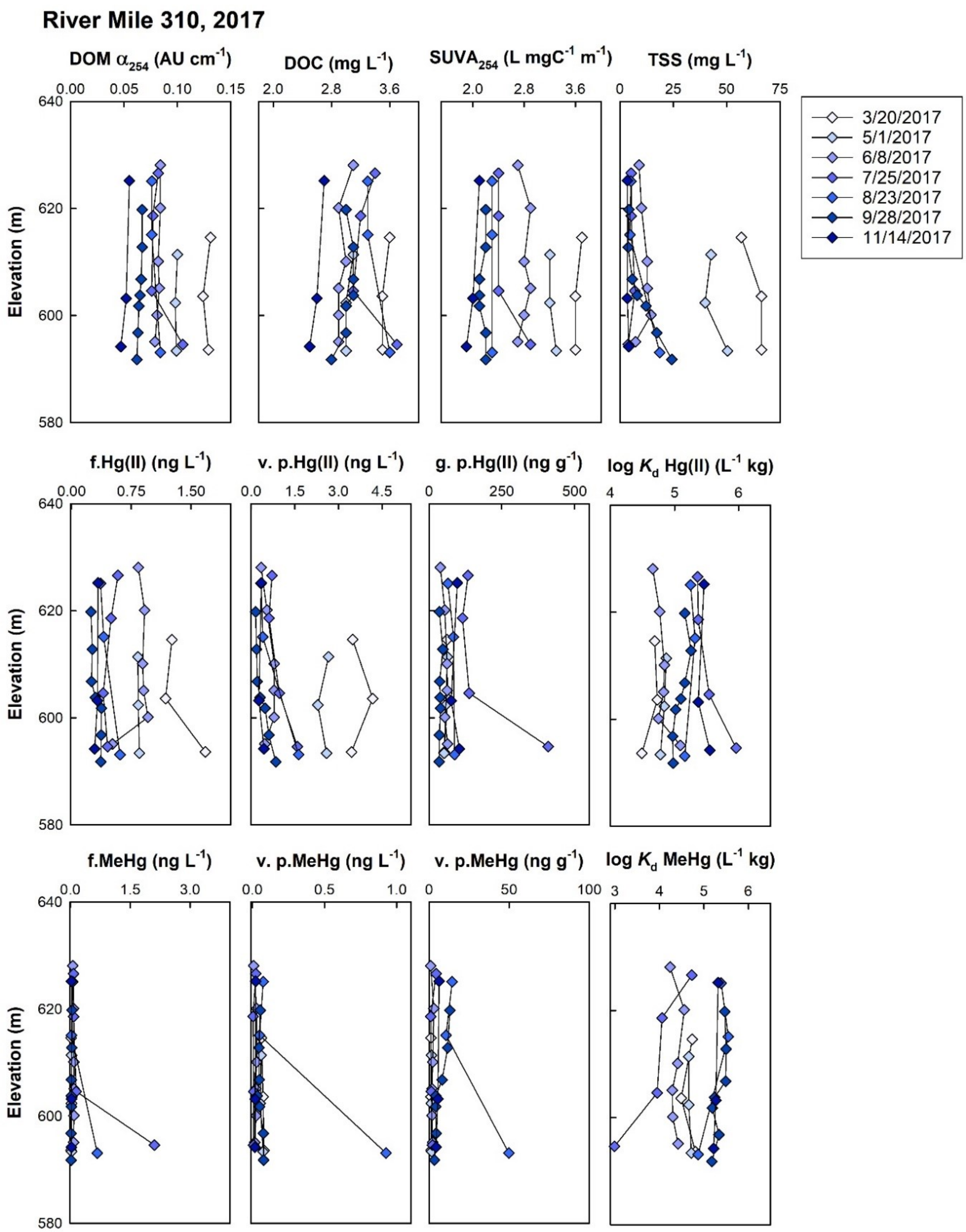

Figure S8. Depth profiles at river mile 310 in Brownlee Reservoir in 2017 of DOM α_{254}, DOC, SUVA$_{254}$, and [TSS] (top panel); f.Hg(II), vol. and grav. p.Hg(II) (ng L^{-1}, ng g^{-1}), and log K_d Hg(II) (middle panel); and f.MeHg, vol. and grav. p.MeHg (ng L^{-1}; ng g^{-1}), and log K_d MeHg (bottom panel).[3] The sediment elevation at RM 310 was 587.6 m.

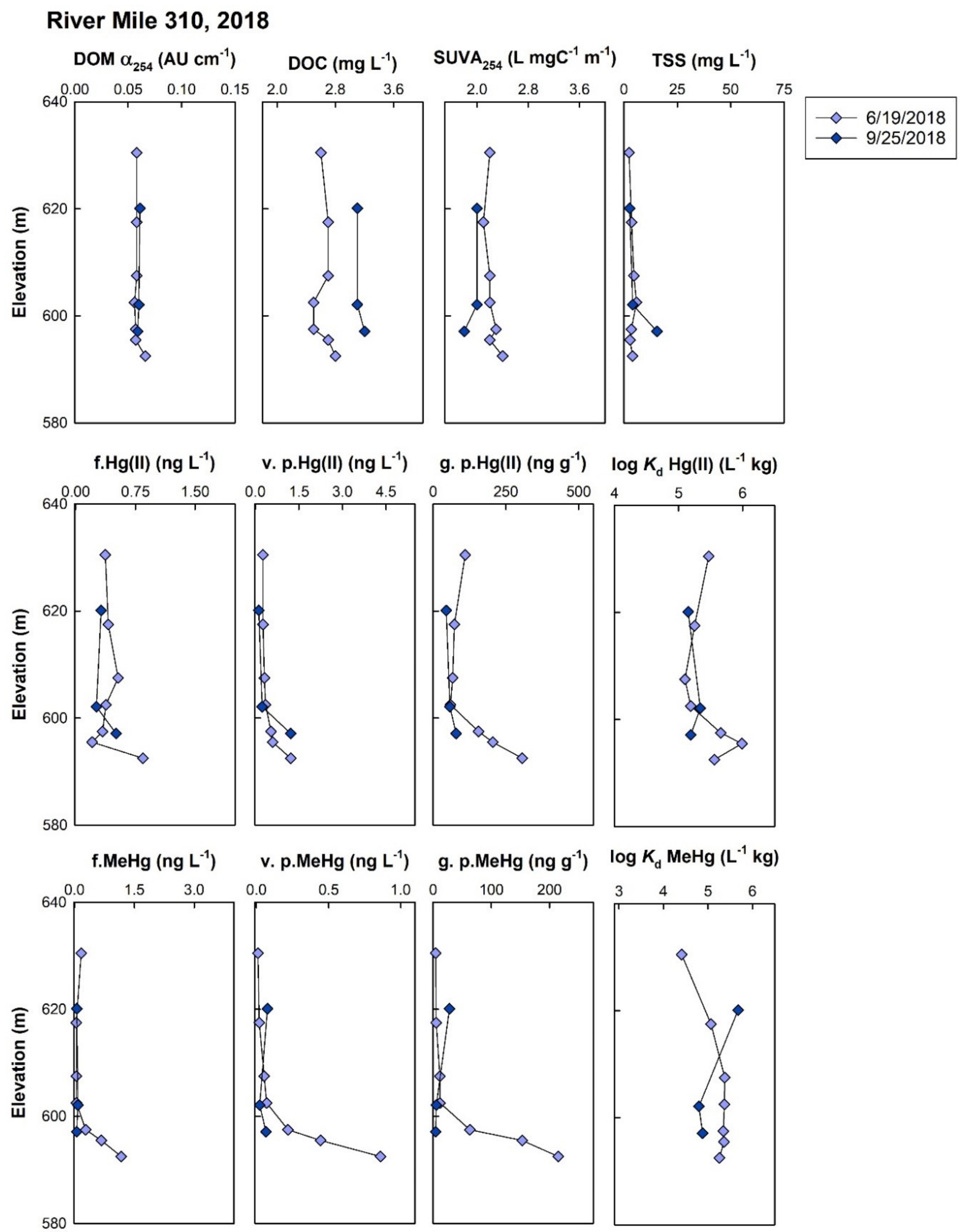

Figure S9. Depth profiles at river mile 310 in Brownlee Reservoir in 2018 of DOM α_{254}, DOC, SUVA$_{254}$, and [TSS] (top panel); f.Hg(II), vol. and grav. p.Hg(II) (ng L^{-1}, ng g^{-1}), and log K_d Hg(II) (middle panel); and f.MeHg, vol. and grav. p.MeHg (ng L^{-1}; ng g^{-1}), and log K_d MeHg (bottom panel).[3] The sediment elevation at RM 310 was 587.6 m.

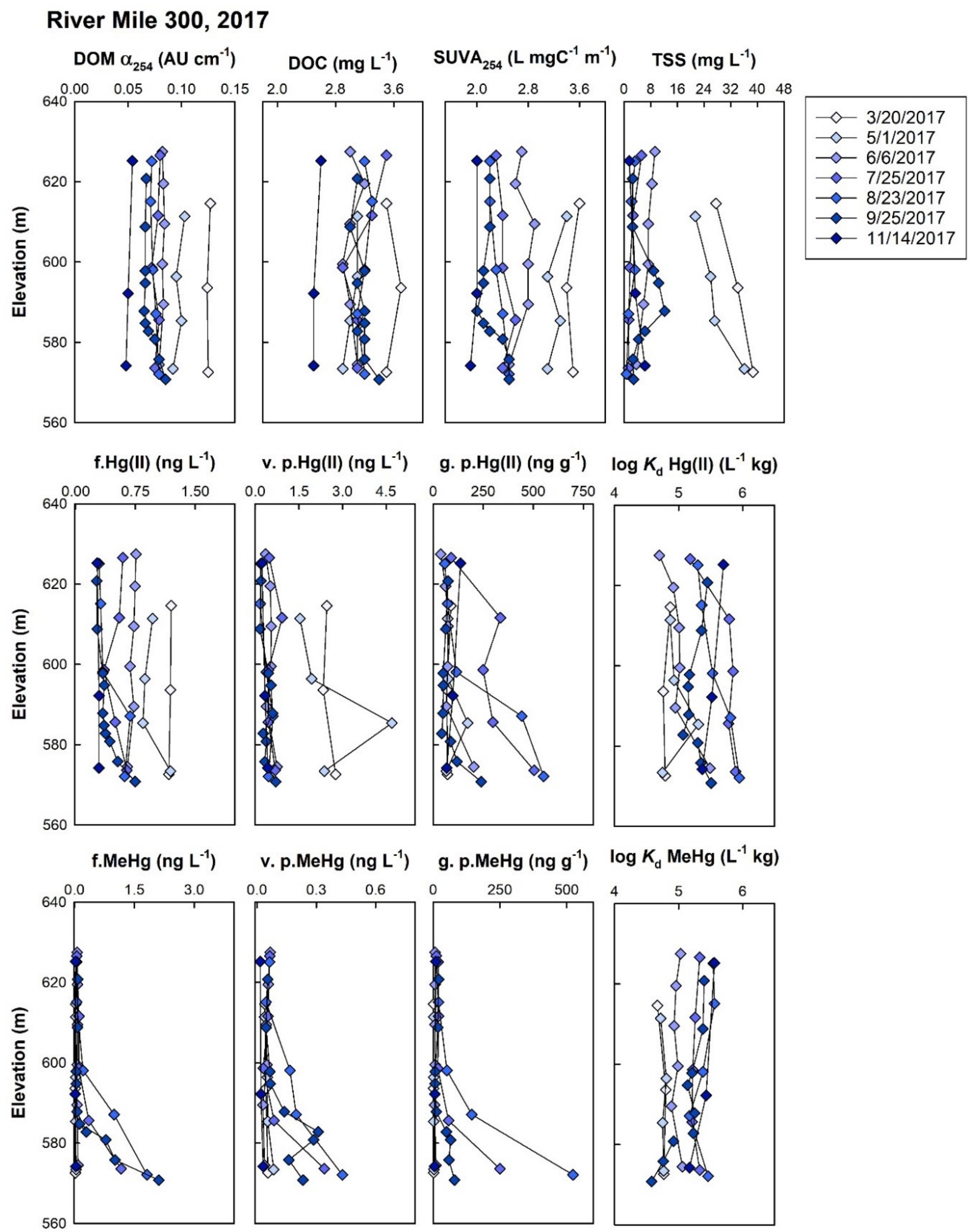

Figure S10. Depth profiles at river mile 300 in Brownlee Reservoir in 2017 of DOM α_{254}, DOC, SUVA$_{254}$, and [TSS] (top panel); f.Hg(II), vol. and grav. p.Hg(II) (ng L^{-1}, ng g^{-1}), and log K_d Hg(II) (middle panel); and f.MeHg, vol. and grav. p.MeHg (ng L^{-1}; ng g^{-1}), and log K_d MeHg (bottom panel).[3] The sediment elevation at this location was 566.6 m.

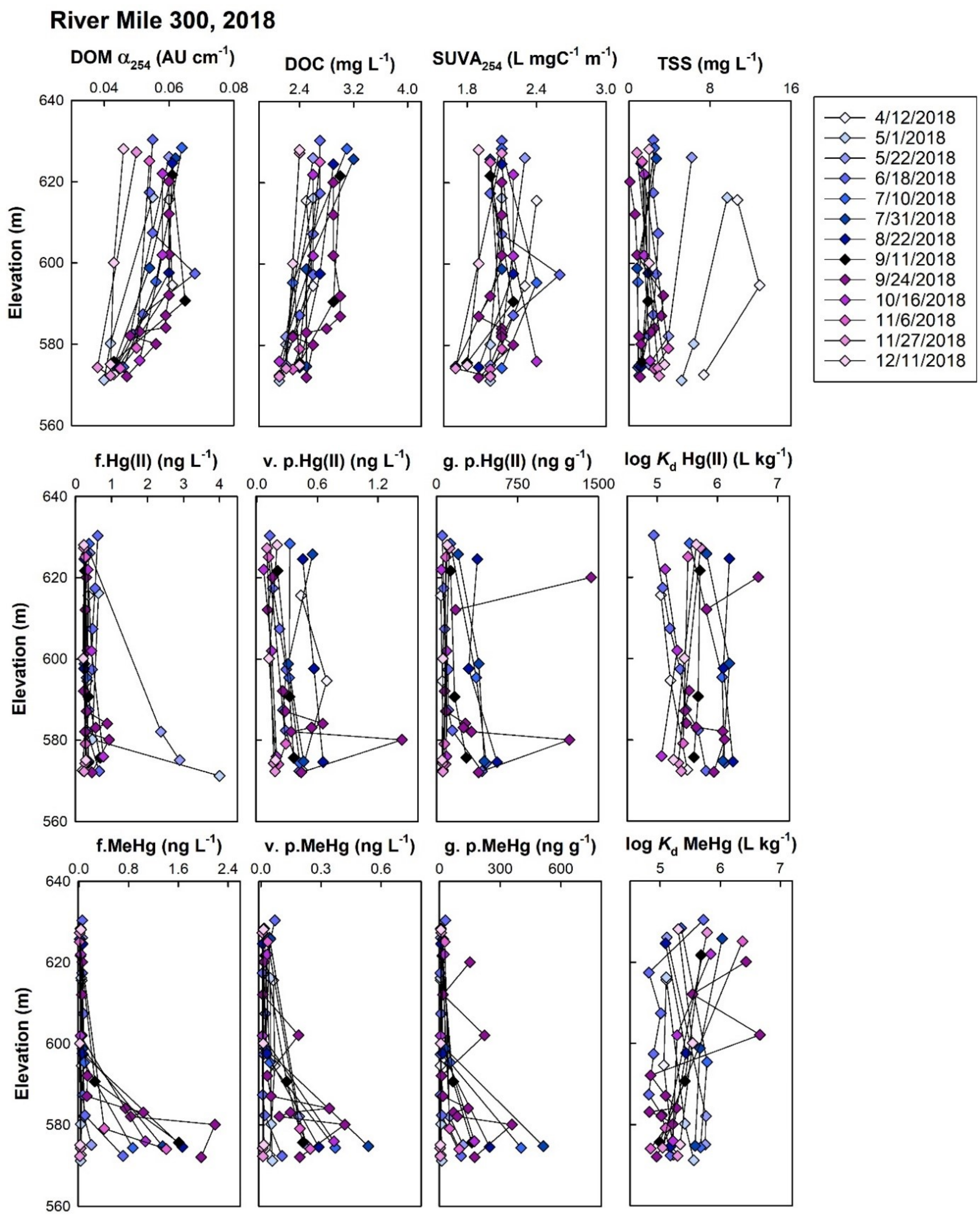

Figure S11. Depth profiles at river mile 300 in Brownlee Reservoir in 2018 of DOM α_{254}, DOC, $SUVA_{254}$, and [TSS] (top panel); f.Hg(II), vol. and grav. p.Hg(II) (ng L^{-1}, ng g^{-1}), and log K_d Hg(II) (middle panel); and f.MeHg, vol. and grav. p.MeHg (ng L^{-1}; ng g^{-1}), and log K_d MeHg (bottom panel).[3] The sediment elevation at this location was 566.6 m.

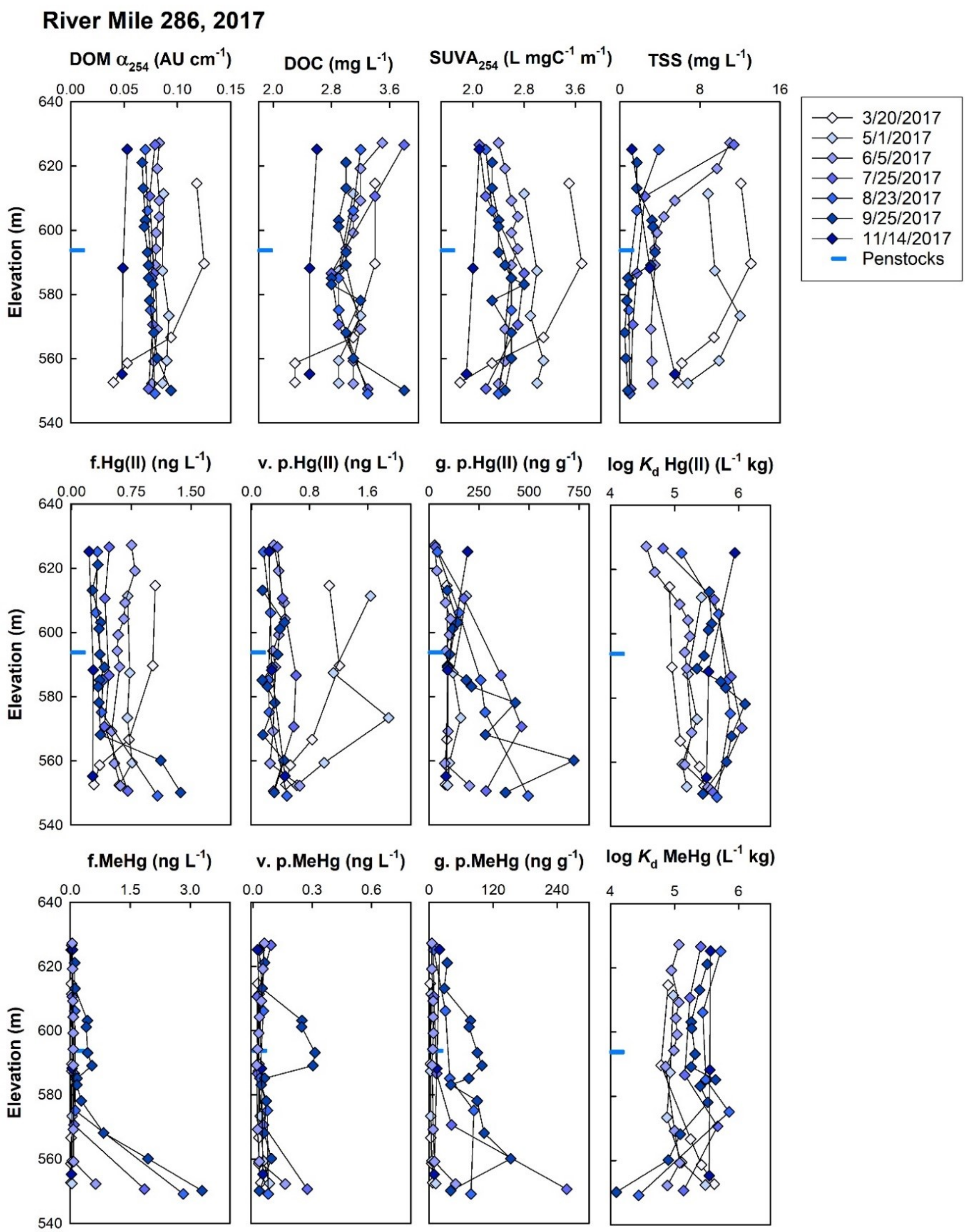

Figure S12. Depth profiles at river mile 286 in Brownlee Reservoir in 2017 of DOM α_{254}, DOC, $SUVA_{254}$, and [TSS] (top panel); f.Hg(II), vol. and grav. p.Hg(II) (ng L^{-1}, ng g^{-1}), and log K_d Hg(II) (middle panel); and f.MeHg, vol. and grav. p.MeHg (ng L^{-1}; ng g^{-1}), and log K_d MeHg (bottom panel).[3] The sediment elevation at this location was 544.6 m and the penstock elevation of Brownlee Dam was 593.75 m.

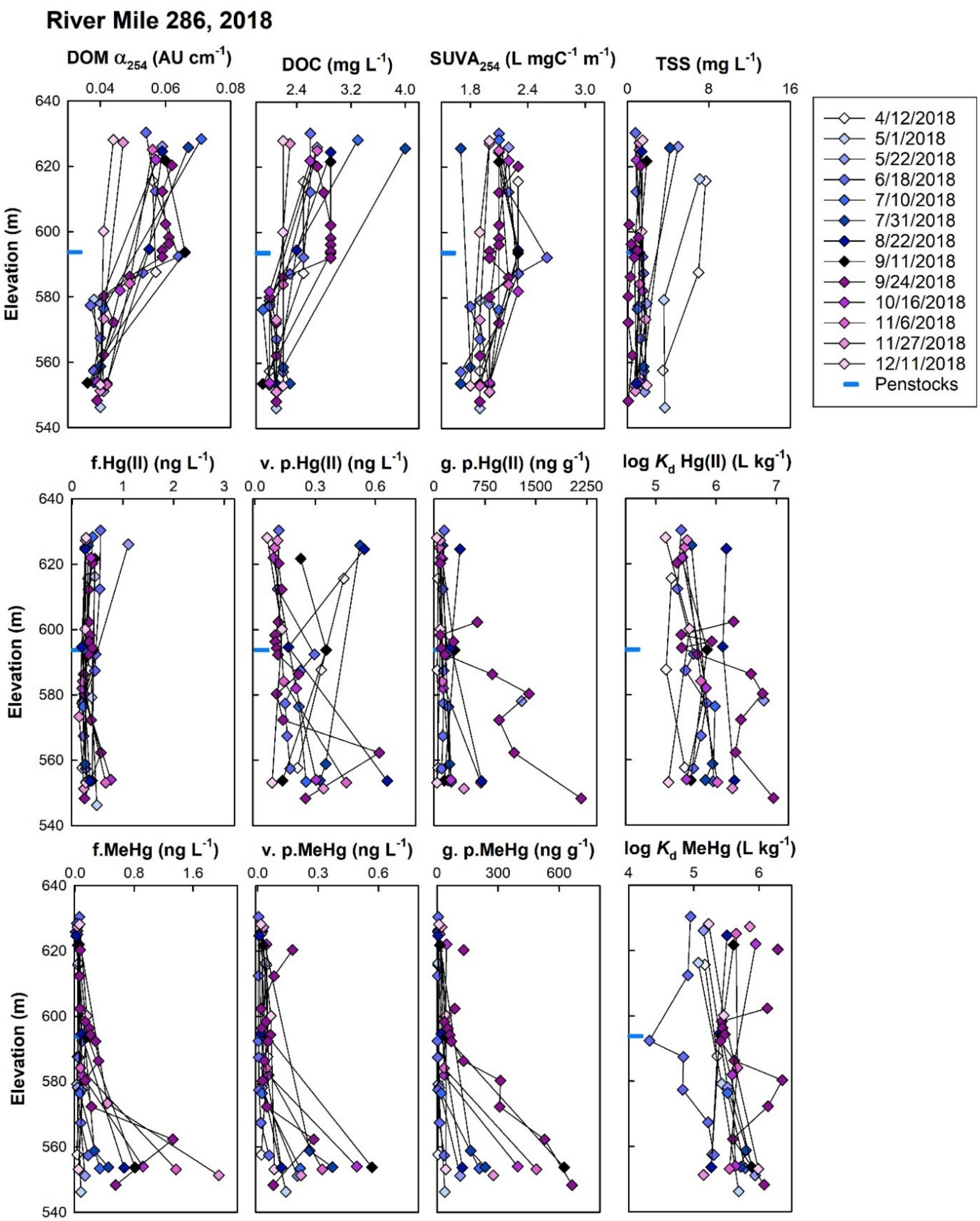

Figure S13. Depth profiles at river mile 286 in Brownlee Reservoir in 2018 of DOM α_{254}, DOC, $SUVA_{254}$, and [TSS] (top panel); f.Hg(II), vol. and grav. p.Hg(II) (ng L^{-1}, ng g^{-1}), and log K_d Hg(II) (middle panel); and f.MeHg, vol. and grav. p.MeHg (ng L^{-1}; ng g^{-1}), and log K_d MeHg (bottom panel).[3] The sediment elevation at this location was 544.6 m and the penstock elevation of Brownlee Dam was 593.75 m.

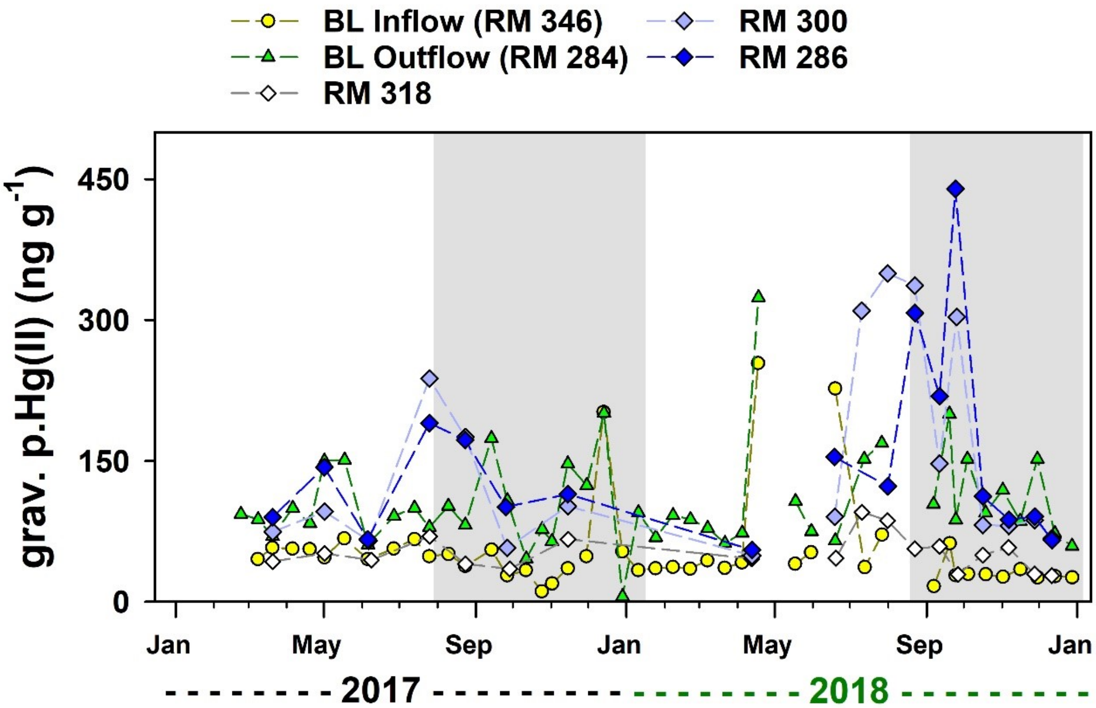

Figure S14. Gravimetric particulate Hg(II) concentration (ng g^{-1}) at the inflow and outflow of Brownlee Reservoir (BL Inflow and Outflow) compared with volume-weighted concentrations within the reservoir at river miles 318, 300, and 286 (2017 – 2018).[3] The gray shaded areas identify the approximate times of reservoir destratification (defined in Table S1). The volume-weighted data are summarized in Table S2.

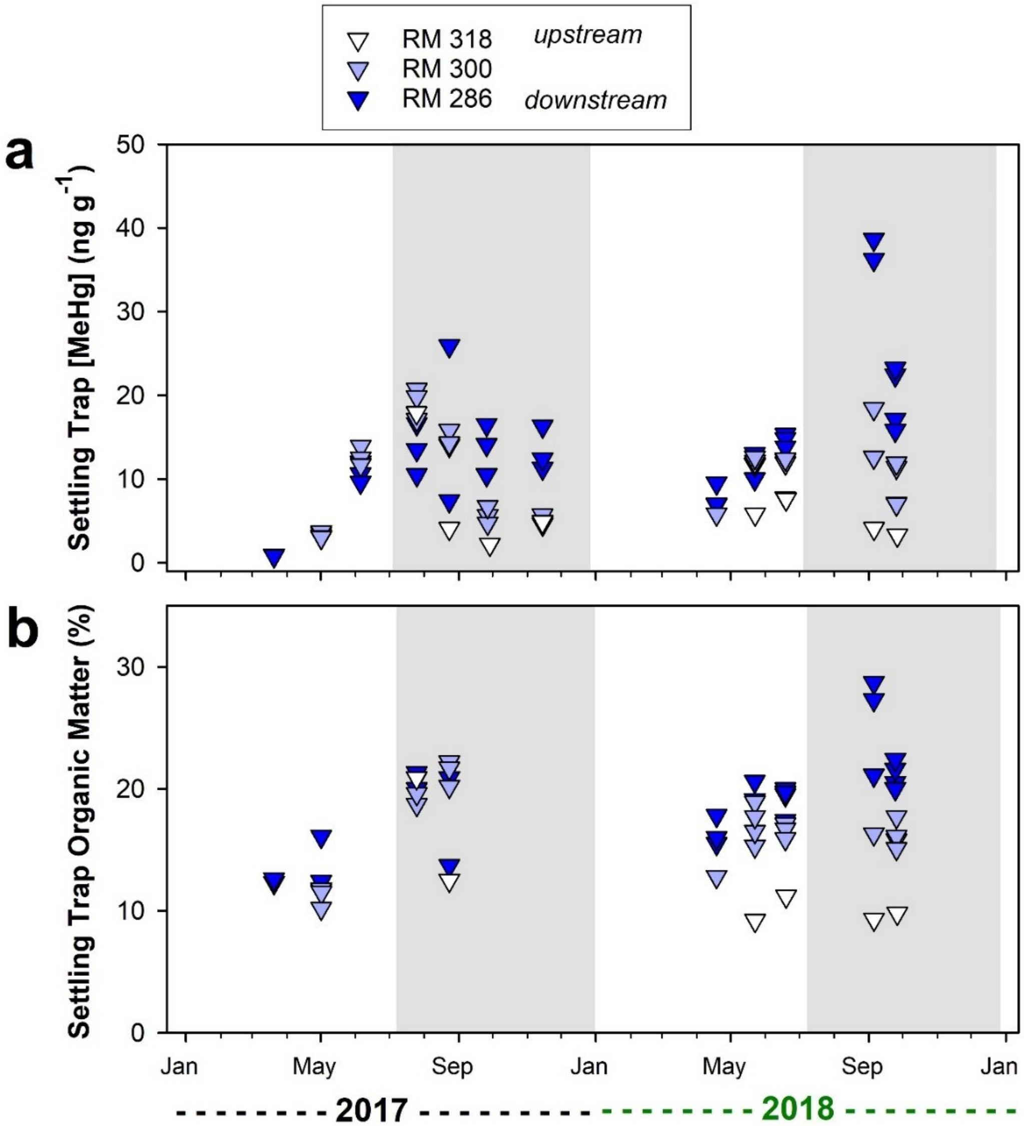

Figure S15. Temporal trends in settling trap material (a) organic matter content (by loss on ignition) and (b) MeHg concentration (ng g^{-1}) between 2017 and 2018 at river miles 318, 300, and 286 in Brownlee Reservoir. Multiple data points at a given time reflect settle trap material collected at varying depths in the water column (see details in supporting data release).[3] The gray shaded areas identify the approximate timeframe of reservoir destratification (defined in Table S1). Settling traps were deployed for 2 weeks, and the collection date is presented for data in the figure.

References

(1) Botelho, D. A.; Imberger, J. Dissolved Oxygen Response to Wind-Inflow Interactions in a Stratified Reservoir. *Limnol. Oceanogr.* **2007**, *52* (5), 2027–2052. DOI: 10.4319/lo.2007.52.5.2027.

(2) Baldwin, A. K.; Eagles-Smith, C. A.; Willacker, J. J.; Poulin, B. A.; Krabbenhoft, D. P.; Naymik, J.; Tate, M. T.; Bates, D.; Gastelecutto, N.; Hoovestol, C.; Larsen, C.; Yoder, A. M.; Chandler, J.; Myers, R. In-Reservoir Physical Processes Modulate Aqueous and Biological Methylmercury Export from a Seasonally Anoxic Reservoir. *Environ. Sci. Technol.* **2022**, *56* (19), 13751–13760. DOI: 10.1021/acs.est.2c03958.

(3) Poulin, B. A.; Breitmeyer, S.E. Krabbenhoft, D. P.; Tate, M. T.; DeWild, J. F.; Ogorek, J. M.; Babiarz, C. L.; Janssen, S. E.; Marvin-DiPasquale, M. C.; Agee, J. L.; Kakouros, E.; Kieu, L.; Arias, M.; Conaway, C.; Antweiler, R. C.; Baldwin, A. K.; Yoder, A.; Clark, G. M.; Aiken, G. R. Chemical Characterization of Water and Suspended Sediment of the Snake River and Hells Canyon Complex (Idaho, Oregon). *U.S. Geol. Surv. data release* **2022**, *ver. 2.0*.

(4) Naymik, J.; Larsen, C.; Myers, R.; Hoovestol, C.; Gastelecutto, N.; Bates, D. Long-Term Trends in Inflowing Chlorophyll A and Nutrients and Their Relation to Dissolved Oxygen in a Large Western Reservoir. *Lake Reserv. Manag.* **2023**, *39* (1), 53–71. https://doi.org/10.1080/10402381.2022.2160395.

(5) U.S. Geological Survey. **2021**, USGS Water Data for the Nation: U.S. Geological Survey National Water Information System Database. Accessed January, 1, 2021. DOI: 10.5066/F7P55KJN.